Analysis of Electric Field and Polarization of SF6 Circuit Breaker to Approach a Suitable Structure

V. Abbasi* and A. Gholami*

Abstract: The application of electric field theory to widely different aspects of electrical insulation has led to more understanding the phenomena**.** Electric fields may be considered as the main reason for insulation failure**.** The purpose of this paper is to modify importance of analyzing electric field in insulation design. The SF6 circuit breaker is chosen as case study that encounters critical situations during its application. The other phenomena affects insulation is the presence of polar species in a non-polar molecular material locally modifies the polarization energy, thus creating local states (traps) on neighboring molecules. Results of calculations carried out for arrays of spatially connected dipoles indicating that local states of a considerable density may be created, modifying the density-of-states function, and therefore influencing the effective mobility of charge carriers. The main result of polarization during application in circuit breaker is loss of life. In this paper the reduction of negative effects of electric field and polarization by choosing a suitable insulation structure in a 33 kV SF6 circuit breaker according to calculation in critical areas is investigated that can also be studied in other types of circuit breakers.

Key words: Polarization, SF6, Chamber, Transient Recovery Voltage (TRV).

1 Introduction

When a circuit breaker operates and the contacts of the breaker are separated, a lot of physical mechanisms such as the gas convection, heat conduction, radiation, and the Lorentz force occur in the chamber [1]. These mechanisms are related to the electric field and polarization. The investigation in chamber is helpful for the designers to improve the performance of breakers [2]. In plasma, the flow, electric, and magnetic fields interact with each other. Accordingly changing one of them affects the others, especially in critical areas in where the maximum values occur that play the main role in breakdown and loss of life [3-5]. Diagnose of maximum values of electric field and polarization is the most important part of analysis to redesign insulation structure.

The field distribution in circuit breaker is non-uniform on a boundary of solid insulation and it makes calculation hard. To overcome this problem finite element method (FEM) is used. Because of sharp edges in solid insulation near contacts (the maximum values occur over them), the redesign process mainly focuses on them to control negative effects. When circuit breaker opens completely voltage between electrodes is more than the other positions, thus it is selected as the worst case for computation. A 33 kV SF6 circuit breaker is considered as the case study and the investigation is performed in four different solid insulation structures to elaborate on the mentioned issue.

Iranian Journal of Electrical & Electronic Engineering, 2010.
Paper first received 13 Sep 2009 and in revised form 23 Jan. 2010.
* The Authors are with the Center of Excellence for Power System Automation and Operation, Iran University of Science and Technology, 16844, Narmak, Tehran, Iran.
E-mails: V_Abbasi@iust.ac.ir, A.Gholami@iust.ac.ir

2 Field Charging

In field charging, ions are transported to suspended particles along the field lines. When electric field increases in some areas the direction and also migration velocity of particles changed leading to making dipolar zones that extremely influence on critical situations. The Coulomb force of a suspended charged particle in an electric field is as follows:

$$F=qE \tag{1}$$

where F is the Coulomb force (N), q is the particle charge (C) and E is the electric field. The viscous force on a moving particle is given by the following equation [3]:

$$F_s = \frac{3\pi\mu d_p \omega_e}{C_m} \tag{2}$$

The particles are moved towards the collecting electrode with a velocity ω_e [3]:

$$\omega_e = \frac{qEC_m}{3\pi\mu d_p} \quad (3)$$

$$C_m = 1 + 2.54\left(\frac{\lambda}{d_p}\right) + 0.8\left(\frac{\lambda}{d_p}\right)\exp\left(\frac{-0.55d_p}{\lambda}\right) \quad (4)$$

$$\lambda = 6.61\times10^{-8}\left(\frac{T}{293}\right)\left(\frac{101.3\times10^3}{P}\right) \quad (5)$$

where ω_e is the migration velocity (m/sec.), μ is the viscosity (Pa.s), d_p is the diameter of particle (m), C_m is the Cunningham correction factor, λ is the mean free path of gas molecules (m), T is the temperature (K), and P is the pressure (Pa). Furthermore, the correction factor C_m is necessary to account for viscosity. When field charging is applicable, the migration velocity is written as [6]:

$$\omega_e = \frac{qE}{3\pi\mu d_p} = \frac{\varepsilon_0\varepsilon_s}{\mu(\varepsilon_s+2)}d_pE^2 \quad (6)$$

The Eq. (6) indicates that velocity is related to quadratic of electric field that verifies our discussion in previous section.

3 Polarization Density in Maxwell's Equations

The behavior of electric fields (E and D), magnetic fields (B, H), charge density (ρ) and current density (J) are described by Maxwell's equations. The role of the polarization density P is described below.

3.1 Relations Between E, D and P

The polarization density P defines the electric displacement field D as:

$$D = \varepsilon_0 E + P \quad (7)$$

Here ε_0 is electric constant. A relation between P and E exists in many materials, as will be described later in next sections.

Bound charge: Electric polarization corresponds to a rearrangement of the bound electrons in the material, which creates an additional charge density, known as the bound charge density ρ_b [7]:

$$\rho_b = -\nabla P \quad (8)$$

So that the total charge density that enters Maxwell's equations is given by:

$$\rho = \rho_f + \rho_b \quad (9)$$

where ρ_f is the free charge density (describing charges brought from outside). At the surface of the polarized material, the bound charge appears as a surface charge density:

$$\sigma_b = P.\hat{n}_{out} \quad (10)$$

where $\hat{n}_{out}$ is the normal vector. If P is uniform inside the material, this surface charge is the only bound charge. When the polarization density changes with time, the time-dependent bound-charge density creates a polarization current density of:

$$J_b = \frac{\partial P}{\partial t} \quad (11)$$

So that the total current density that enters Maxwell's equations is given by:

$$J = J_f + \nabla\times M + \frac{\partial P}{\partial t} \quad (12)$$

where J_f is the free-charge current density, and the second term is the magnetization current density (also called the bound current density), a contribution from atomic-scale magnetic dipoles (when they are present).

3.2 Relation Between P and E in Various Materials

In a homogeneous linear and isotropic dielectric medium, the polarization is associated with and proportional to the electric field E. In an anisotropic material, the polarization and the field are not necessarily in the same direction. Then, the i^{th} component of the polarization is related to the j^{th} component of the electric field according to:

$$P_i = \sum_j \varepsilon_0\chi_{ij}E_j \quad (13)$$

where χ is the electric susceptibility tensor of the medium. The case of an anisotropic dielectric medium is described by the field of crystal optics. As in most electromagnetism, this relation deals with macroscopic averages of the fields and dipole density, so that one has a continuum approximation of the dielectric materials that neglects atomic-scale behaviors. The polarizability of individual particles in the medium can be related to the average susceptibility and polarization density by the Clausius-Mossotti relation. In general, the susceptibility is a function of the frequency ω of the applied field. When the field is an arbitrary function of time *t,* the polarization is a convolution of the Fourier transform of $\chi(\omega)$ with the $E(t)$. This reflects the fact that the dipoles in the material cannot respond instantaneously to the applied field, and causality considerations lead to the Kramers–Kronig relations. If the polarization P is not linearly proportional to the electric field E, the medium is termed nonlinear and is described by the field of nonlinear optics. To a good approximation (for sufficiently weak fields, assuming no permanent dipole moments are present), P is usually given by a Taylor series in E whose coefficients are the nonlinear susceptibilities:

$$P_i/\varepsilon_0 = \sum_j \chi_{ij}^{(1)}E_j + \sum_{jk}\chi_{ij}^{(2)}E_jE_k + \sum_{jkl}\chi_{ij}^{(3)}E_jE_kE_l + \dots \quad (14)$$

where $\chi^{(1)}$ is the linear susceptibility, $\chi^{(2)}$ gives the Pockels effect, and $\chi^{(3)}$ gives the Kerr effect.

4 Case Study

In order to study the effect of electric field and polarization in sf6 circuit breaker, indoor technical data of circuit breaker structure is necessary. The case study is a Medium voltage (33 kV) circuit breaker that is show in Fig. 1.

The upper contact is fixed and the lower contact is movable, when the circuit breaker opens (The worst case) the lower contact compresses SF6 gas and it flows between contacts to eliminate arc; however, sometimes it doesn't work accurately. When the contacts open completely transient recovery voltage (TRV) has the most value. Accordingly electric field, polarization and velocity of ions and particles increase intensively helping spark to be reminded or increase the possibility of re-spark. The second reason for spark or re-spark is due to the non uniform distributed electric field in some parts (e.g. upper contact entrance of solid insulation). To distinguish the area of non uniform distributed electric field (critical zones) FEM is used that analyses electric fields based on Maxwell equations. TRV is considered as the input of FEM software (COMSOL). Also, boundary conditions for insulations and contacts are defined accurately. The result of the simulation is shown in Fig. 2.

4.1 Electric Field Analysis

To reduce electric field in the entrance of solid insulation, different structures with various kinds of shape (as shown in Fig. 3) are proposed. Structure 1 and 2 are similar, the only difference between them is the slope of solid insulation in entrance. Also, structure 3 and 4 are similar, the only difference between them is the arc of solid insulation in entrance. For the approach; electric field analysis separately is performed for the proposed structures. The results are shown in Fig. 3(a) and Fig. 3(b).

As shown in Figs. 3(a) and 3(b), the values of electric fields near entrance of the solid insulation in various structures are different. The upper contact and insulation compose dipole with diverse characterize that influence on migration velocity and direction of ions (Eq. 6). The shape of entrance is an important factor which in fact influences on electric field distribution. Slopes and arcs of entrance determine the situation arising from the non-uniform electric field distribution. Thus obtained results need to be more analyzed to choose appropriate structure. Essentially, the last part of the interruption process from various aspects is influenced by the configuration. To demonstrate this matter electric field on boundary of solid insulation is shown in Fig. 4 and electric polarization is discussed in next section.

For structure 2 (Fig. 4(a)) maximum values of electric field occur in a limit region of edge and can be neglected. On the other hand in structure 3 and 4 (Fig. 4(b)) maximum values consist of larger regions. The maximum value of electric field in structure 2 is 5.7×10^5 [V/m] and the colored plot (occurring the most values of electric fields for it) occupied only 2% of entrance area (the values are in the range of (4.5×10^5 [V/m], 5.7×10^5 [V/m]). However, about 88% of structure 2 consist of values in the range of (2×10^5 [V/m], 3.8×10^5 [V/m]). The worst results occur for structure 4: maximum value is 5.3×10^5 [V/m] and the region includes 22% of entrance (the values are in the range of (4.2×10^5 [V/m], 5.3×10^5 [V/m]). Also, 65% of it consists of values in the range of (2×10^5 [V/m], 3.6×10^5 [V/m]). Table 1 contains percentages of electric field values for proposed structures. From the simulation results the appropriate structure can be properly diagnosed.

4.2 Electric Polarization Analysis

Relation between polarization with electric field and dielectric characteristic represents by Eqs. (13) and (14). Accordingly, the best structure from this point of view is (2) that as demonstrated in Fig. 5.

Table 2 includes electric polarization values for proposed structures. The results in this table show that structure 2 is the appropriate choice from polarization point of view. In structure 2 maximum values occur only in 2% of the entrance while the lowest values occur mainly in 88% of the entrance.

Table 1 Electric fields values in different regions of entrance for proposed structures

Structure 1	Percentage of area	4%	21%	75%
	Electric fields 10^5 [V/m]	4.2-5.11	3.6-4.2	2-3.6
Structure 2	Percentage of area	2%	10%	88%
	Electric fields 10^5 [V/m]	4.5-5.7	3.8-4.5	2-3.8
Structure 3	Percentage of area	17%	10%	73%
	Electric fields 10^5 [V/m]	4-5.12	3.2-4	2-3.2
Structure 4	Percentage of area	22%	13%	65%
	Electric fields 10^5 [V/m]	4.2-5.3	3.6-4.2	2-3.6

Table 2 Electric polarization values for different regions of entrance

Structure 1	Percentage of area	4%	21%	75%
	Electric polarization 10^{-6} [C/m^2]	7.2-8.6	6-7.2	3-6
Structure 2	Percentage of area	2%	10%	88%
	Electric polarization 10^{-6} [C/m^2]	7.8-9.6	6-7.8	3-6
Structure 3	Percentage of area	17%	10%	73%
	Electric polarization 10^{-6} [C/m^2]	7-8.6	6-7	3-6
Structure 4	Percentage of area	22%	13%	65%
	Electric polarization 10^{-6} [C/m^2]	7.1-8.92	6.2-7.1	3.18-6.2

Fig. 1 structure of a typical 33 kV circuit breaker

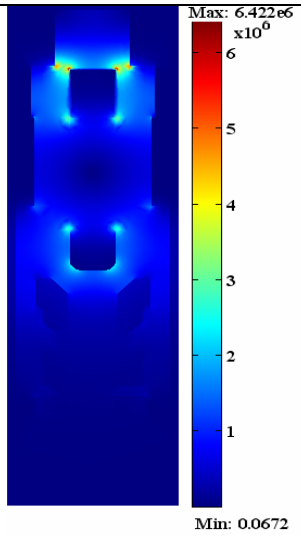

Fig. 2 Computation of electric field in chamber

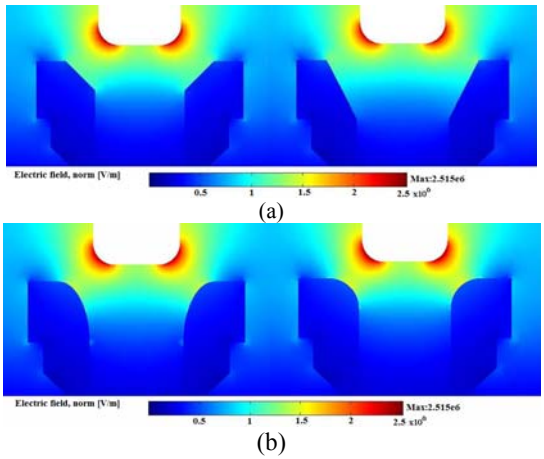

Fig. 3 Computation of electric field in chamber near entrance of solid insulation (critical zones). (a) structure 1 and 2, (b) structure 3 and 4

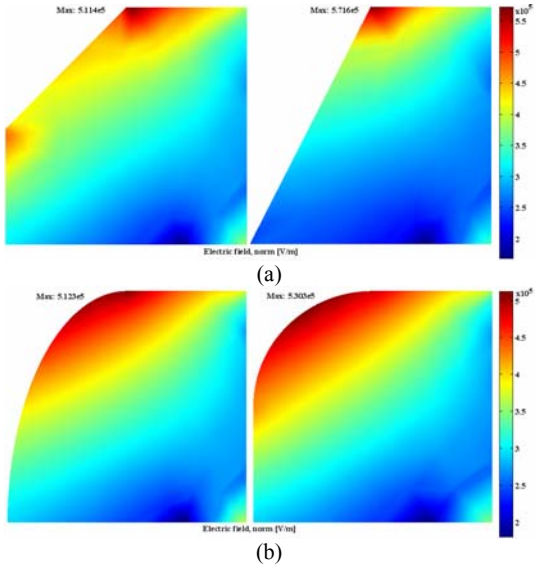

Fig. 4 Computation of electric field in one side of entrance of solid insulation. (a) structure 1 and 2, (b) structure 3 and 4

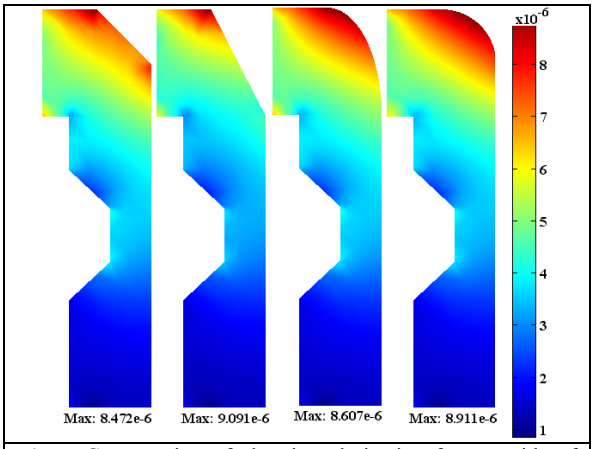

Fig. 5 Computation of electric polarization for one side of solid insulation_ structure 1, 2, 3 and 4

4.3 Electric Field and Space Charge Analysis

When hot gas flows, it increases the possibility of dielectric Breakdown during the transient recovery voltage after clearing. As the gas temperature increases, the breakdown field of the gas decreases and the energy required to heat the gas to a conducting state decreases as well. However, the maximum energy available from the electric field (determined by the breakdown field of the gas) goes as the square of the field and therefore drops rapidly as the withstand field of the gas drops with increasing temperature. Thus, analyzing electric field and space charge can be useful for predicting re-ignition in different structures during the transient recovery voltage after clearing. High values of electric field and space charge on the boundary of the nozzle's entrance increases the possibility of re-ignition. To simulate the electric field and space charge Convection

and diffusion, Electrokinetic flow, Electrostatic and Fluid flow equations are coupled.

Convection and diffusion of the analyte: The material balance of the analyte comes from the equation:

$$\delta_{ts}\frac{\partial c}{\partial t}+\nabla\cdot(-D\nabla c)=R-u\cdot\nabla c \qquad (15)$$

The equation (15) gives the material balance in a non-conservative form, because the flow field is divergence-free. In this equation D denotes the diffusion coefficient, R represents the reaction rate, and δ_{ts} is Time-scaling coefficient. Here *R* equals zero because no reactions take place in the bulk of the fluid, only on the reaction surface.

Electrokinetic flow: Electrokinetic flow affects the process by equation (16).

$$\delta_{ts}\frac{\partial C}{\partial t}+\nabla\cdot(-D\nabla c-zu_m FC\nabla V)=R-ug\nabla C \qquad (16)$$

where C is the concentration, δ_{ts} is Time-scaling coefficient, *R* represents the reaction rate, u_m is the mobility, z is the charge number, u is the r-velocity, and V is the potential.

Electrostatic: General electrostatic equation is used as shown in equation (17).

$$-\nabla\cdot\left(\left(\sigma+\frac{\varepsilon_0\varepsilon_r}{T}\right)\nabla V-J^e\right)=\frac{p_0}{T} \qquad (17)$$

where σ is the electrical conductivity, ε_r is the relative permittivity, p_0 is the space charge density, and J^e is the external current density.

Fluid flow: Fluid flow analysis is used to calculate velocity in different steps. The fluid flow is described by the Navier-Stokes equations as:

$$\rho\frac{\partial u}{\partial t}-\nabla.\eta\left(\nabla u+(\nabla u)^T\right)+\rho u.\nabla u+\nabla P=0$$
$$\nabla.u=0 \qquad (18)$$

where ρ is the density (kg/m^3), u is the velocity vector (m/s^{-1}), η is the viscosity (N.s/m^2), and P is the pressure (Pa).

In this part, equations 15, 16, 17 and 18 are coupled in this part to calculate electric field and space charge. Input of the simulation is TRV curve which is considered linear. Nonlinear input usually causes not-converging, while linear curve can be used with a first order approximation. Approximated values are consistent with our above discussion. The results of the simulation for structures 2 and 3 are shown in Figs. 6 and 7.

Space charge changes magnitude and the shape of distribution of electric filed on the boundary of solid insulation-structure by producing electric filed. For structure 2 (Fig. 6) maximum values of electric field occur in a limit region of edge which can be neglected. On the other hand, for structure 3 maximum values are higher than values of the prior structure. The obtained results of the previous section are confirmed with these simulation results, especially for the results of the 4-1. Furthermore, electric field affects ionization as shown in Fig. 7, the values of space charge density in the most part of structure 3 is higher than structure 2. Therefore, structure 2 provides better characteristics to be chosen as appropriate structure in comparison with the others.

4.4 Aging Analysis

Electric field affects insulation life, especially in the case of non-uniform electric filed distribution. To analysis aging based on electric field, the region bearing the maximum value should be recognized. In the previous subsection (4-1) the non-uniform electric fields are categorized in Table 1 for the proposed structures that can be used for aging analysis. The relation between electric field and aging can be written as the following equations [8, 9, 10]:

$$L=c\zeta^{-n} \qquad (19)$$

$$L=Ae^{\left(\frac{E-\sigma\zeta}{KT}\right)} \qquad (20)$$

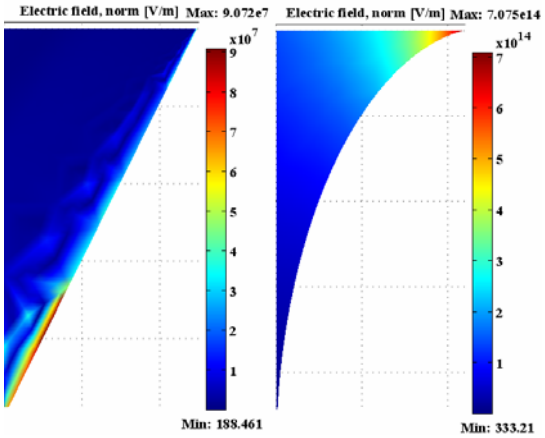

Fig. 6 Computation of electric field on the boundary of entrance of solid insulation-structures 2 and 3

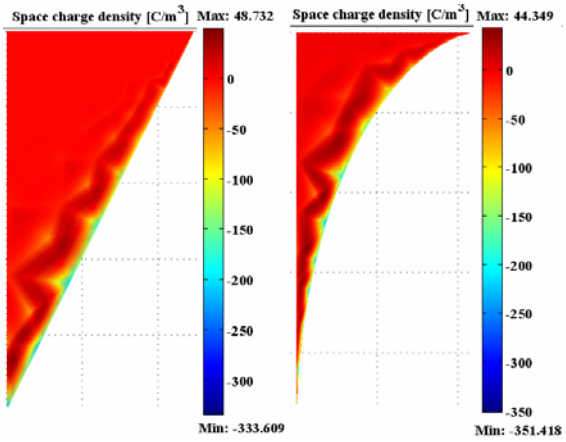

Fig. 7 Computation of space charge on the boundary of solid insulation-structures 2 and 3

where L is the age of insulation; c, n and A are constant related to insulation characteristic ($9 \prec n \prec 12$); E is the activation energy; T is the temperature; σ is the conductivity and ζ is the electric field. Equation (20) is used for electro thermal analysis; thus, equation (19) is useful in this part. Comparing the proposed structures with each other from this point of view, the rate of aging insulation between structures can be obtained. The maximum value of electric field for structure 2 is 5.7×10^5 [V/m] and for structure 3 is 5.12×10^5 [V/m], so, the rate of age is 2.62 ($\frac{L_{st3}}{L_{st2}} = 2.62$).

The simulation is performed for the time interval in which the circuit breaker is open. Although, the result is noticeable, the time interval is short in most case studies and can be approximately neglected. In some medium voltage circuit breakers interruptions occur several times during their life's time. Accordingly, their aging should be considered in the proposed structures. To improve aging in structure 2, the edges can be replaced by small arcs in attempt to reduce electric field.

5 Conclusion

In interruption process various phenomena occur that should be analyzed to prevent main faults in circuit breaker. When the interruption is complete, the most value of voltage appears on contacts leading to increase the possibility of spark. Although SF6 has proper insulation characters, breakdown arises in some situations. Enhancing electric field in some areas of circuit breaker causes to increase the rate of polarization. Thus the direction and migration velocities of ions change. The space between upper contact and entrance of solid insulation is the critical region (in the case study). To better operation of circuit breaker, a new practical structure is proposed. In structure 2 polarization, space charge and also electric field in most part of the entrance of solid insulation reduced considerately. The research work can open new scopes in the area of circuit breaker structure (the others point of view analysis complete it) that are based on restructuring the solid insulation part of circuit breaker.

Reference

[1] Liu X., Tang T., Cao Y., Zhao Y. and Huang D., "Performance Analysis of High Voltage SF6 Circuit Breaker based on Coupling Computation of Electric-Gas Flow Field," *IEEE Automation Congress*, WAC, pp. 1-4, 2008.

[2] Wu Y., Rong M., Li J. and Lou J., "Calculation of Electric and Magnetic Fields in Simplified Chambers of Low-Voltage Circuit Breakers," *IEEE Transactions on Magnetics*, Vol. 42, No. 4, pp. 1007-1010, 2006.

[3] Mizuno A., "Electrostatic Precipitation," *IEEE Transactions on Dielectrics and Electrical Insulation*, Vol. 7, No. 5, pp. 615-624, 2000.

[4] McAllister W., "Electric Fields and Electrical Insulation," *IEEE Transactions on Dielectricsand Electrical Insulation*, Vol. 9, No. 5, pp. 672-696, 2002.

[5] Robin-Jouan P., Dufournet D. and Montillet G. F., "Digital Analysis of the Breakdown Process in High-Voltage Circuit Breakers," *IEEE Transmission and Distribution Conference*, pp. 986-991, 2006.

[6] White H. J., *Industrid Electrostntic Precipitation*, Addison-Wesley Publishing Co., 1962.

[7] Saleh B. E. A., Teich M. C., *Fundamentals of Photonics*, Hoboken, NJ: Wiley. pp. 154, 2007.

[8] Pandey S. B., "Estimation for a Life Model of Transformer Insulation under Combined Electrical & Thermal stress," *IEEE Transaction on reliability*, Vol. 41, No. 3, pp. 466-468, 1992.

[9] Endicott H. S., Hatch B. D., Sohmer R. G., "Application of Eyring Model to Capacitor Aging Data", *IEEE Trans. Component parts*, Vol. 12, No. 4, pp. 34-41, 1965.

[10] Ramu T. S., "On the Estimation of Life Power Apparatus Insulation under Combined Electrical and Thermal Stress", *IEEE Trans. Electrical insulation*, Vol. 20, No. 6, pp. 70-78, 1985.

Vahid Abbasi has received his B.Sc. degree in electrical engineering in 2002 from Shahid Chamran University, Ahvaz, Iran, and the M.Sc. degree in electrical engineering in 2004 from the Iran University of Science and Technology, Tehran, Iran, where he is currently working toward the Ph.D. degree. His current research interests include HV circuit breakers, electromagnetic compatibility considerations in electrical power systems and insulation coordination.

Ahmad Gholami has received his B.Sc. Degree in electrical engineering from IUST, Tehran, Iran, in 1975, the M.Sc. and PhD. Degrees in electrical engineering from UMIST, Manchester, England, in 1986 and 1989 respectively. He is currently an associate professor in the Electrical Engineering Department of Iran University of Science and Technology. His main research activities are high voltage engineering, electrical insulation, insulation coordination, transmission lines and substations planning.